International Journal of Science and Research Archive
eISSN: 2582-8185
Cross Ref DOI: 10.30574/ijsra
Journal homepage: https://ijsra.net/

(RESEARCH ARTICLE)

Check for updates

Exploring the Potentials of GC-MS Identified Compounds in a Fraction of *Raphia hookeri* (Rh) Against Transforming Growth Factor Receptor (TGF-B1): An *In Silico* Approach

John Akighir [1,*], James Ojochenemi Yakubu [2], Ayu Agbecha [3] and Reuben Owuna [4]

[1] *Department of Chemical Science, College of Sciences and Education, University of Mkar, Mkar P.M.B. 017, Gboko Benue State, Nigeria.*
[2] *Department of Biochemistry, Faculty of Natural and Applied Sciences, Federal University Wukari 200 Katsina-Ala Road, P.M.B 1020 Wukari, Taraba State, Nigeria.*
[3] *Department of Medical Laboratory Science, College of Health Sciences, Rev. Fr. Moses Orshio Adasu University Makurdi, Benue State, Nigeria.*
[4] *Department of Laboratory Sciences, Hospitals Management Board, Makurdi-Aliade Road, Makurdi, Benue State, Nigeria.*

International Journal of Science and Research Archive, 2026, 19(02), 751-772

Publication history: Received on 02 April 2026; revised on 11 May 2026; accepted on 13 May 2026

Article DOI: https://doi.org/10.30574/ijsra.2026.19.2.0993

Abstract

Background: TGF-β I play a crucial role in liver fibrosis progression, with its activation linked to the up-regulation of pro-fibrotic genes and proteases. Hence, the research focuses on analyzing the bioactive compounds present in a fraction of *Raphia hookeri* using GC-MS analysis to target the TGF-β type I receptor. Methods: Gas Chromatography-Mass Spectrometry (GC-MS), absorption, distribution, metabolism, excretion (ADME) and oral toxicity studies were performed. Molecular docking studies were conducted using Maestro software, followed by validation using the MMGBSA method. GC-MS analysis revealed 26 compounds belonging to various classes. The ADME and oral toxicity study also revealed the drug-likeness characters of the compounds. Results:In the molecular docking analysis, Benzenebutanal, gamma.,4-dimethyl- revealed a binding affinity of -5.926 (Kcal/Mol) when compared with Galunisertib (control) (-10.210 (Kcal/Mol).The MMGBSA post docking score also revealed -53.47 and -82.51 Kcal/Mol respectively. Hydrogen bond interactions (distance Å) of TGF-β type I receptor with Benzenebutanal, gamma, 4-dimethyl- (Asp351 (1.90, 2.08) and Galunisertib (control) (Tyr249 (1.88), Asp351 (1.90) further supported the finding. Conclusion: Benzenebutanal, gamma, 4-dimethyl- may be a promising compound for hepatoprotection. However, further in vivo and in vitro exploration of the lead compound as potential drug candidates targeting TGF-β type I receptor is imperative.

Keyword*: Raphia hookeri;* TGF-β I; Gas Chromatography-Mass Spectrometry (GC-MS); Molecular docking

1. Introduction

Transforming growth factor (TGF-β) super family consists of 33 multifunctional cytokines, among which TGF-β1 is the most abundant, and well-studied (Schon and Weiskirchen, 2014). Research indicates that TGF-β1 plays a crucial role in liver fibrosis progression, with its activation linked to the up-regulation of pro-fibrotic genes and proteases (Link *et al.,* 2023). Studies have shown that inhibiting TGF-β1 and its downstream pathways can alleviate liver fibrosis by blocking it's binding to receptors and inhibiting fibrosis-related processes (Xudong *et al.,* 2022). Furthermore, inhibition of TGF-β1 signaling has been found to accelerate regeneration in fibrotic livers, improve liver function, and ameliorate fibrosis, highlighting TGF-β1 as a promising therapeutic target in liver diseases (Bo *et al.,* 2021). Additionally, inhibiting TGF-β1

* Corresponding author: Akighir J

has been shown to reduce senescence-induced impairment of liver regeneration, further supporting its hepatoprotective effects (Thomas *et al.,* 2018).

Galunisertib (LY2157299 monohydrate) is an oral small molecule inhibitor of the TGF-β receptor I kinase that specifically down regulates the phosphorylation of SMAD2, abrogating activation of the canonical pathway. Furthermore, galunisertib has antitumor activity in tumor-bearing animal models such as breast, colon, lung cancers, and hepatocellular carcinoma (Herbertz *et al.*, 2015)

Raphia hookeri (Rh) commonly known as Raphia palm belongs to the Family: The *Palmaceae* family includes monocotyledonous plants frequently found in West Africa, particularly in the lowlands and swampy regions of north-central Nigeria, where they can grow in water up to a meter deep (Akighir *et al*., 2023). Raffia palm roots are utilized in various medicinal applications. In traditional medicine, the root extract is commonly used to create a laxative and to relieve stomach pain in infants (Akpan and Usoh, 2004). Various experimental models have investigated the effects of Raffia palm (*Raphia hookeri*) leaf extract on enzymes linked to type-2 diabetes mellitus (T2DM) and pro-oxidant induced oxidative stress in rat pancreas (Mbaka *et al.,* 2012 and Dada *et al.,* 2017). Not much is known about the fruit (mesocarp) though; it is used as a forest food. Hence, the research focuses on analyzing the bioactive compounds found in a fraction of *Raphia hookeri* using GCMS analysis to target the TGF-β type I receptor.

2. Materials and methods

2.1. Sample Collection

The fruits of *R. Hookeri* were collected along River Buruku in Benue State. The identification and authentication of the plant material with voucher number RH 206 was done by Dr. J. Ojobo of Botany Department, Joseph Sarwuan Tarka University, Makurdi, Benue State, Nigeria. The plant material was critically examined for any disease and only the healthy fruits were selected for use. The fruits were dehulled, and the thin yellow mesocarp extracted. The material was thoroughly rinsed and air-dried at room temperature and was pulverized to fine powder using laboratory manual blender (Ncube *et al*., 2008; Nguyen*et al*., 2017).

2.2. Sample Extraction

Sample extraction was done according the method adopted by Yakubu *et al.* 2014 and Ipav *et al*. (2022) with little modifications. About four hundred (400 g) of powered plant material was soaked in 1600 mL of ethanol and was agitated intermittently for 48 hours. The mixture was first filtered with cheese cloth, then Whatman No 1 filter paper. The filtrates were concentrated using rotary evaporator at reduced pressure and was preserved in moisture-free, airtight laboratory containers, then stored in the refrigerator at 4ºC for further use.

2.3. Fractionation of Ethanolic Fruit Extract of *R. hookeri*

The ethanol extract was subjected to column chromatograph to separate the extract into its component fractions. Silica gel ($G_{60\text{-}120}$ mesh size) was used in packing the column while different solvent combinations based on increasing polarity as the mobile phase

2.4. Packing of Column

The column packing procedure followed the methodology outlined by Yakubu *et al*. (2014). Glass wool was placed at the bottom of the glass column using a glass rod. The slurry was prepared by dissolving 75 g of silica gel in 180 mL of absolute chloroform. This slurry was used to pack the chromatographic column, which had dimensions of 30 mm in diameter and 400 mm in height, ensuring that the solvent could flow freely into a conical flask placed below. The packing process was considered successful when the solvent drained without carrying any silica gel or glass wool into the tap. After packing, the tap was sealed, and the column was left to stabilize for 24 hours. Subsequently, the clear solvent at the top of the silica gel was allowed to drain down the silica gel meniscus.

2.5. Elution

The method of Akighir *et al.* (2023) was adopted with little modifications. The ethanolic fruit extract (2 g) was dissolved in 15 mL absolute n-hexane and the solution was applied unto the chromatographic column. Elution of the extract was done with the solvent system of gradually increasing polarity, starting with n-Hexane, Chloroform, Ethyl acetate, Methanol, Ethanol and Distilled water. The following ratio of solvent combinations was sequentially used in the elution process.

Solvent Combination	Ratios
n-Hexane: Chloroform	100 : 0, 80 : 20, 60 : 40, 40 : 60, 20 : 80
Chloroform: Ethyl acetate	100 : 0, 80 : 20, 60 : 40, 40 : 60, 20 : 80
Ethyl acetate: Methanol	100 : 0, 80 : 20, 60 : 40, 40 : 60, 20 : 80
Methanol: Ethanol	100 : 0, 80 : 20, 60 : 40, 40 : 60, 20 : 80
Ethanol: Distilled water	100 : 0, 80 : 20, 60 : 40, 40 : 60, 20 : 80
Distilled water	100

A measured volume (400 mL) of each solvent combination was poured into the column each time using separatory funnel. The eluted fractions were collected in aliquots of 100 mL using beakers. F_{24} was used for Gas Chromatography-Mass Spectrometry (GC-MS) analysis because; it had the highest antioxidant activity.

2.6. Gas Chromatography-Mass Spectrometry (GC-MS) Analysis

Gas Chromatography-Mass Spectrometry (GC-MS) analysis: This was carried out as described by Thomas *et al*. (2013); Yakubu *et al.* (2019) on a Perkin Elmer Turbo Mass Spectrophotometer (Norwalk, CTO6859 and USA) which includes a Perkin Elmer Auto-sampler XLGC. Analysis was carried out using electron impact ionization at 70 eV and data was evaluated using total ion count (TIC) for compound identification and quantification. The spectrums of the components were compared with the database of the spectrum of known components stored in the GC-MS library. Measurement of peak areas and data processing were carried out by Turbo-Mass-OCPTVS-Demo SPL Software.

2.7. ADME and Protox Prediction

Swiss ADME (*http://www.swissadme.ch/index.php*) was used to profile the physicochemical, lipophilicity, pharmacokinetics, and Lipinski's drug-likeness of 26 ligands. Toxicity assessment was performed on Protox (*http://biosig.unimelb. edu.au/pkcsm/prediction*). All the ligands were compared to the Galunisertib (Control) ligand and ranked based on their ADME profiles to find the top drug-like candidates.

2.8. Protein and Ligand Preparation

2.8.1. Preparation of Protein Structures and Grid Generation

TGF-β type I receptor structure (PDB ID: 1VJY, having resolution <2 Å, R-Value Free <0.30, R-Value Work <0.25) was selected and obtained from Protein Data Bank (http://www.rscb.org) with good resolutions. Protein structure was prepared using protein preparation wizard in Maestro panel. During preparation of protein bond orders were assigned and hydrogen atoms were added as well. Water molecules were removed within 3 Å of het groups (Sinha *et al.,* 2019). Finally, OPLS-2005 force field was applied to minimize the structure of protein (Schrodinger, LLC, NY, USA, 2009) (Halgren *et al.,* 2004). Further receptor grid boxes were generated using "Glide's Receptor Grid Generation" module at the active site (with the radius of 20 Å around the crystal structure) of co-crystallized ligand with the computing cubic box of 10 Å × 10 Å × 10 Å (Jasuja *et al.,* 2014).

2.8.2. Ligand Preparation

A total of 26 compounds were selected to perform the molecular docking studies. PubChem database was used to extract out the 3D chemical structures of the selected molecules. 3D and geometry optimizations with energy minimization of ligands were executed using algorithms monitored in Schrödinger Maestro v 11.4 (Subramaniyan *et al.,* 2018). LigPrep module (Schrodinger, LLC, NY, USA, 2009) was used from the Maestro builder panel to prepare ligand and generate 3D structure of the ligands by adding hydrogen atoms and removing salt and ionizing at pH (7 ± 2) (Modi *et al.,* 2018). Energy minimization was performed using OPLS-2005 force field by using the standard energy function of molecular mechanics and RMSD cut off 0.01 Å to generate the low-energy ligand isomer (Pradeep and Rajanikant 2012) Molecular Docking

Molecular docking is a structure-based drug design approach to identify the essential amino acid interactions between the selected protein and generated ligands with low energy conformation (Carlesso *et al.,* 2019). Minimum interaction of the ligands characterized by the scoring function was used to forestall the binding affinity with the receptor. Glide

Standard precision (SP), docking protocol was applied without smearing any constrain. Concluding energy assessment was done with the dock score. Visualization of docked ligands was done by Maestro interface (Schrödinger Suite, LLC, NY). MMGBSA Calculations

Binding free energies were calculated using MM-GBSA, VSGB 2.0 implicit 754alvation model, and OPLS-2005 via Prime (Lyne *et al.,* 2006). The binding free energy was calculated using the equation:

$\Delta G_{bind} = G_{complex} - G_{protein} - G_{ligand}$

Where, $G_{complex}$, $G_{protein}$, and G_{ligand} represent the free binding energy of the protein-ligand complex; protein; and ligand, respectively.

3. Results

3.1. GC-MS Analysis of the Ethanolic Fruit Extract of *Raphia hookeri*

The GC-SM analysis revealed 26 compounds namely: Heptadecyl acetate, Propanal 2, 3-dihydroxy- (S)-, 6-Oxa-3, 9-dithiaundecane-1, 11-diol, Beta-copaene, Benzenebutanal gamma 4-dimethyl-,Germacrene D, 1, 3-Cyclohexadiene 5-(1, 5-dimethyl-4-hexenyl)-2-methyl, Beta-Bisabolene, Cyclohexene 3-(1, 5-dimethyl 4-hexenyl)-6-methylene, Tetradecane 1-chloro, 2-Butenoic acid 4-hydroxy-methyl ester, 2-Pentadecanol, Oxalic acidcyclobutyltridecyl ester, Imidazole 2-fluoro-5-hydroxy-1-ribofuranosyl, Hexadecanoic acid methyl ester, D-Galactonic acid gamma-lactone, Pentane-1, 2,3,4,5-pentaol, Xylitol, Ribitol, Beta-D-Glucopyranoside methyl 3,6-anhydro-, 1-Decanol 2-ethyl-,5-Methyl-7-amino-s-triazolo(1,5-a)pyrimidine, 2-Heptadecanol,17-Pentatriacontene, Supraene and Alpha D-Glucose.1, 3-Cyclohexadiene, 5-(1, 5-dimethyl-4-hexenyl)-2-methylrevealed the highest area percentage of 21.3405 and a retention time of 10.578.

Table 1 GC-MS Analysis of the Compounds Identified from Ethanolic Fruit Extract of *Raphia hookeri*

Name of Compound	**Molecular formula**	**Molecular weight (g/mol)**	**Structure**
Heptadecyl acetate	$C_{19}H_{38}O_2$	298.5	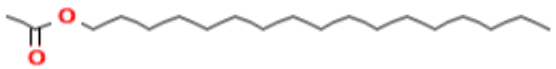
Propanal 2,3-dihydroxy-, (S)-	$C_3H_6O_3$	90.08	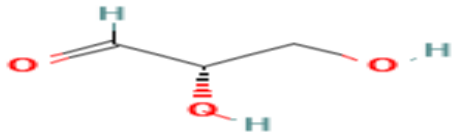
6-Oxa-3,9-dithiaundecane-1,11-diol	$C_8H_{18}O_3S_2$	226.4	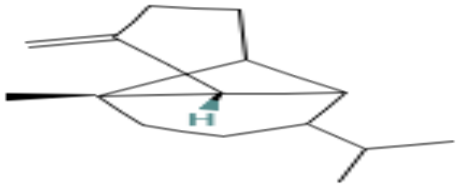
beta-copaene	$C_{15}H_{24}$	204.35	
Benzenebutanal gamma ,4dimel-	$C_{12}H_{16}O$	176.25	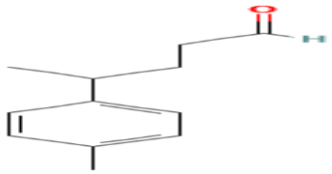

Germacrene D	$C_{15}H_{24}$	204.35	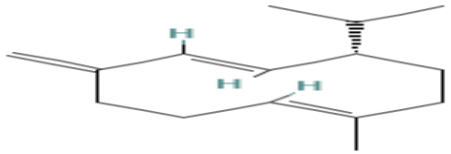
1,3-Cyclohexadiene, 5-(1,5-dimethyl-4-hexenyl)-2-methyl-	$C_{15}H_{24}$	204.35	
beta-Bisabolene	$C_{15}H_{24}$	204.35	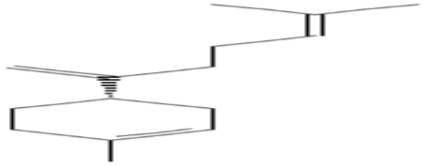
Cyclohexene 3-(1,5-dimethyl-4-hexenyl)-6-methylene-	$C_{15}H_{24}$	204.35	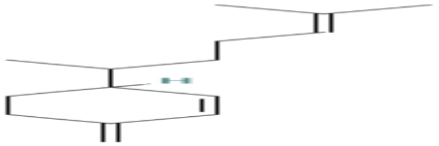
Tetradecane 1-chloro-	$C_{14}H_{29}Cl$	232.83	
2-Butenoic acid 4-hydroxy-, methyl ester	$C_5H_8O_3$	116.11	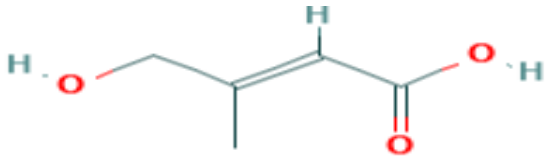

2-Pentadecanol	$C_{15}H_{32}O$	228.41	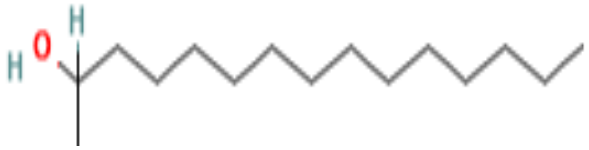
Oxalic acid cyclobutyltridecyl ester	$C_{19}H_{34}O_4$	326.5	
Imidazole, 2-fluoro-5-hydroxy-1-ribofuranosyl-	$C_8H_{11}FN_2O_5$	234.18	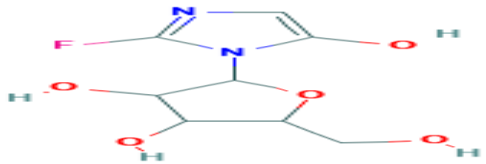
Hexadecanoic acid, methyl ester	$C_{17}H_{34}O_2$	270.5	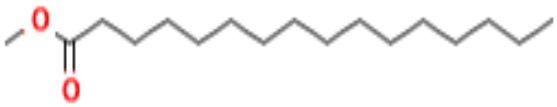
D-Galactonic acid, .gamma.-lactone	$C_6H_{10}O_6$	178.14	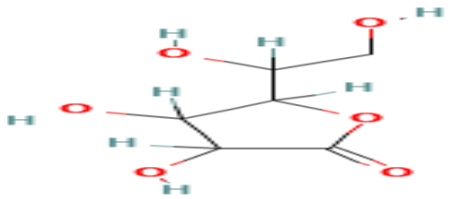

Pentane-1,2,3,4,5-pentaol	$C_{10}H_{20}O_7$	252.26	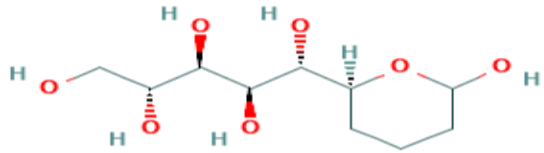
Xylitol	$C_5H_{12}O_5$	152.15	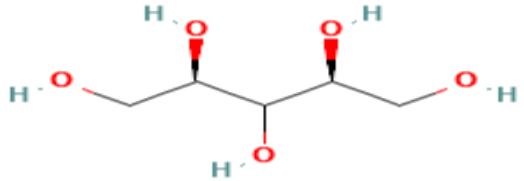
Ribitol	$C_5H_{12}O_5$	152.15	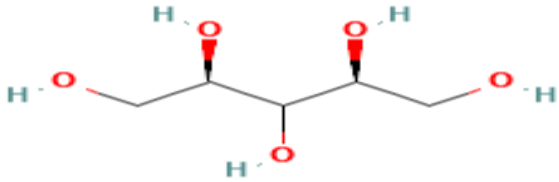
beta-D-Glucopyranoside, methyl 3,6-anhydro-	$C_7H_{12}O_5$	176.17	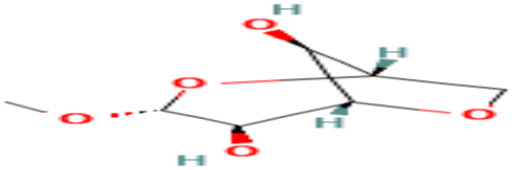
1-Decanol, 2-ethyl-	$C_{12}H_{26}O$	186.33	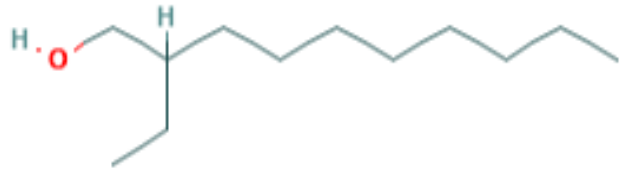

5-Methyl-7-amino-s-triazolo(1,5-a)pyrimidine	$C_6H_7N_5$	149.15	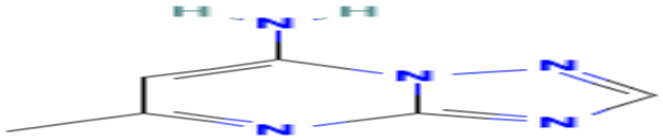
2-Heptadecanol	$C_{17}H_{36}O$	256.5	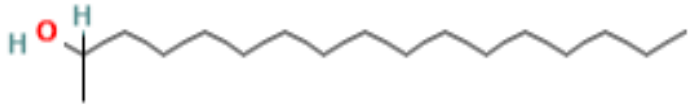
17-Pentatriacontene	$C_{35}H_{70}$	490.9	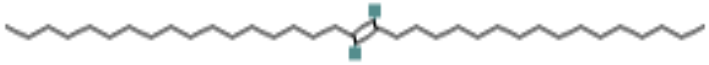
Supraene	$C_{30}H_{50}$	410.7	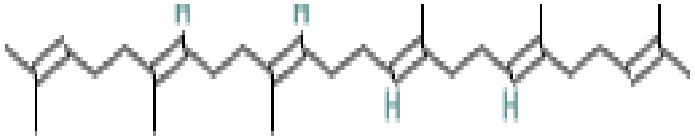
alpha-D-Glucose	$C_6H_{13}O_9P$	260.14	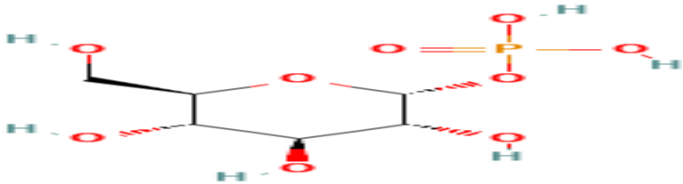

Table 2 Oral Toxicity Predications of Ligands

Name of Compound	LD_{50} mg/kg	Toxic Class	Hepatotoxicity	Carcinogenicity	immunotoxicity	Mutagenicity	Cytotoxicity
Heptadecyl acetate	3000	5	Inactive	Inactive	Inactive	Inactive	Inactive
Propanal, 2,3-dihydroxy-, (S)-	200	3	Inactive	Inactive	Inactive	Inactive	Inactive
6-Oxa-3,9-dithiaundecane-1,11-diol	4920	5	Inactive	Inactive	Inactive	Inactive	Inactive
.beta.-copaene	4700	5	Inactive	Inactive	Inactive	Inactive	Inactive
Benzenebutanal, gamma.,4-dimethyl-	2580	5	Inactive	Inactive	Inactive	Inactive	Inactive
GermacreneD	5300	5	Inactive	Inactive	Active	Inactive	Inactive
1,3-Cyclohexadiene, 5-(1,5-dimethyl-4-hexenyl)-2-methyl-, [S-(R*,S*)]-	1680	4	Inactive	Inactive	Inactive	inactive	Inactive
beta.-Bisabolene	4400	5	Inactive	Inactive	Inactive	Inactive	Inactive
Cyclohexene, 3-(1,5-dimethyl-4-hexenyl)-6-methylene-, [S-(R*,S*)]-	5000	5	Inactive	Inactive	Inactive	Inactive	Inactive
Tetradecane, 1-chloro-	7340	6	Inactive	Inactive	Inactive	Inactive	Inactive
2-Butenoic acid, 4-hydroxy-, methyl ester	1410	4	Inactive	Inactive	Inactive	Inactive	Inactive
2-Pentadecanol	1000	4	Inactive	Inactive	Inactive	Inactive	Inactive
Oxalic acid, cyclobutyltridecyl ester	5000	5	Inactive	Inactive	Inactive	Inactive	Inactive
Imidazole, 2-fluoro-5-hydroxy-1-ribofuranosyl-	3390	5	Inactive	Inactive	Inactive	Inactive	Inactive
Hexadecanoic acid, methyl ester	5000	5	Inactive	Inactive	Inactive	Inactive	Inactive
D-Galactonic acid, gamma.-lactone	10700	6	Inactive	Inactive	Inactive	inactive	inactive
Pentane-1,2,3,4,5-pentaol	23000	6	Inactive	Inactive	Inactive	Inactive	Inactive
Xylitol	12500	6	Inactive	Inactive	Inactive	Inactive	Inactive

Ribitol	12500	6	Inactive	Inactive	Inactive	Inactive	inactive
beta.-D-Glucopyranoside, methyl 3,6-anhydro-	684	3	Inactive	Inactive	Inactive	Inactive	inactive
1-Decanol, 2-ethyl-	1000	4	Inactive	Inactive	Inactive	Inactive	inactive
5-Methyl-7-amino-s-triazolo(1,5-a)pyrimidine	414	4	Inactive	Active	Inactive	Inactive	Inactive
2-Heptadecanol	1000	4	Inactive	Inactive	Inactive	Inactive	Inactive
17-Pentatriacontene	2760	5	Inactive	Inactive	Inactive	Inactive	Inactive
Supraene	5000	5	Inactive	Inactive	Inactive	Inactive	Inactive

LD50: Lethal Dose of 50, Toxicity class 1: fatal if swallowed (LD50 ≤ 5), Toxicity class 2: fatal if swallowed (5 < LD50 ≤ 50), Toxicity class 3: toxic if swallowed (50 < LD50 ≤ 300), Toxicity class 4: harmful if swallowed (300 < LD50 ≤ 2000), Toxicity class 5: may be harmful if swallowed (2000 < LD50 ≤ 5000), Toxicity class 6: non-toxic (LD50 > 5000).

Table 3 ADME Properties of Ligands Identified by GC-MS Analysis

Name of Compound	**A**	**B**	**C**	**D**	**E**	**F**	**G**	**H**	**I**	**J**	**K**	**L**	**M**
Heptadecyl acetate	2	0	6.28	17	High	No	No	Yes (1)	yes	no	no	no	No
Propanal, 2,3-dihydroxy-, (S)-	3	2	-1.03	2	High	No	No	No(0)	no	no	no	no	No
6-Oxa-3,9-dithiaundecane-1,11-diol	3	2	0.98	10	High	No	No	No	no	no	no	no	No
beta.-copaene	0	0	4.40	1	Low	Yes	No	Yes(1)	yes	yes	yes	no	No
Benzenebutanal, .gamma.,4-dimethyl-	1	0	2.97	4	High	yes	No	No	no	no	no	yes	No
Germacrene D	0	0	4.30	1	Low	No	No	Yes(1)	no	no	yes	no	No
1,3-Cyclohexadiene, 5-(1,5-dimethyl-4-hexenyl)-2-methyl-, [S-(R*,S*)]-	0	0	4.47	4	Low	No	No	Yes(1)	no	yes	yes	no	No
beta.-Bisabolene	0	0	4.83	4	Low	No	No	Yes(1)	no	no	yes	no	No
Cyclohexene, 3-(1,5-dimethyl-4-hexenyl)-6-methylene-, [S-(R*,S*)]-	0	0	4.56	4	Low	No	No	Yes(1)	no	yes	yes	no	No
Tetradecane, 1-chloro-	0	0	5.86	12	Low	No	No	Yes(1)	yes	no	no	no	No
2-Butenoic acid, 4 hydroxy-, methyl ester	3	1	0.16	3	High	No	No	No	yes	no	no	no	Yes

2-Pentadecanol	1	1	5.04	12	High	Yes	No	No	No	No	Yes	No	No
Oxalic acid, cyclobutyltridecyl ester	4	0	5.21	16	High	Yes	No	No	No	No	No	No	Yes
Imidazole, 2-fluoro-5-hydroxy-1-ribofuranosyl-	7	4	-1.13	2	High	No	No	No	No	No	No	No	No
Hexadecanoic acid, methyl ester	2	0	5.54	15	High	Yes	No	Yes(1)	Yes	No	No	No	No
D-Galactonic acid, .gamma.-lactone	6	4	-1.79	2	Low	No	No	No	No	No	no	no	No
Pentane-1,2,3,4,5-pentaol	7	6	-1.79	5	Low	no	Yes	Yes(1)	No	No	No	no	No
Xylitol	5	5	-1.76	4	Low	no	No	no	No	No	No	no	No
Ribitol													
Cyclohexanol, 1R-4-acetamido-2,3-cis-epoxy-													
.beta.-D-Glucopyranoside, methyl 3,6-anhydro-	5	2	-0.87	1	High	no	No	no	No	no	no	no	No
1-Decanol, 2-ethyl-	1	1	3.84	9	High	yes	no	no	no	no	no	no	No
5-Methyl-7-amino-s-triazolo(1,5-a)pyrimidine	3	1	0.18	0	High	no	no	no	yes	no	no	no	No
2-Heptadecanol	1	1	5.76	14	high	no	no	yes	no	no	yes	no	No
17-Pentatriacontene	0	0	13.13	31	Low	No	Yes	Yes	no	no	no	no	No
Supraene	0	0	9.38	15	Low	No	No	Yes	no	no	no	no	No
alpha.-D-Glucose	9	6	-2.96	3	Low	No	Yes	Yes	no	no	no	no	No

A: Num. H-bond acceptors, B: Num. H-bond donors, C: Consensus Log $P_{o/w}$, D: Num. Rotatable bonds, E: GI absorption, F: BBB permeant, G: P-gp Substrate, H: Lipinski Druglikeness, I: CYP1A2 inhibitor, J: CYP2C19 inhibitor, K: CYP2C9 inhibitor, L: CYP2D6 inhibitor, M: CYP3A4 inhibitor

Table 4 Docking Scores and Interactions

Name of Compounds	Docking Score(Kcal/mol)	Interactions with Hydrogen Bonds and Distance (Å)
Heptadecyl acetate	-0.915	Lys232 (2.21)
Propanal, 2,3-dihydroxy-, (S)-	-3.721	Tyr249*(1.88,2.11)
6-Oxa-3,9-dithiaundecane-1,11-diol	-0.487	Ile211(1.81), Ser280(1.91)
beta.-copaene	-5.991	NONE
Benzenebutanal, .gamma.,4-dimethyl-	-5.926	Asp351*(1.90,2.08)
1,6-Naphthyridine	-7.041	His283(2.01)
Germacrene D	-4.957	None
1,3-Cyclohexadiene, 5-(1,5-dimethyl-4-hexenyl)-2-methyl-, [S-(R*,S*)]-	-4.036	None
beta.-Bisabolene	-5.424	NONE
Cyclohexene, 3-(1,5-dimethyl-4-hexenyl)-6-methylene-, [S-(R*,S*)]-	-4.153	None
Tetradecane, 1-chloro-	-0.645	None
2-Butenoic acid, 4-hydroxy-, methyl ester	-4.453	His283(1.90),Ile211(1.89)
2-Pentadecanol	-0.188	Ile211(1.92)
Oxalic acid, cyclobutyltridecyl ester		
Imidazole, 2-fluoro-5-hydroxy-1-ribofuranosyl-	-6.083	Asp351*(1.86,1.81,1.90), Lys337(2.09)
Hexadecanoic acid, methyl ester	-0.110	None
D-Galactonic acid, .gamma.-lactone	-5.105	Asp351*(1.66,1.75),Lys213(2.14),Lys337(2.11,2.48)
Pentane-1,2,3,4,5-pentaol	-3.568	Asp351*(1.85,1.66),Lys337(1.84,2.08),Asn338(2.16)
Xylitol	-3.568	Asp351*(1.85,1.66),Lys337(1.84,2.08), Asn338(2.16)
Ribitol	-3.568	Asp351*(1.85,1.66),Lys337(1.84,2.08), Asn338(2.16)
beta.-D-Glucopyranoside, methyl 3,6-anhydro-	-5.340	Asp351* (1.83),Lys337(1.92)

1-Decanol, 2-ethyl-	-1.099	His283(2.10)
5-Methyl-7-amino-s-triazolo(1,5-a)pyrimidine	-7.441	His 283 (2.13, 2.20)
2-Heptadecanol	-0.194	His283(2.01)
Supraene	-3.731	None
Galunisertib (Control)	-10.210	Tyr249*(1.88), Asp351*(1.90)

*Interactions Common with the Control

Table 5 Rescoring Docking of Ligands and Control Using MMGBSA

Name of Compound	**Docking Score (Kcal/Mol)**	**MMGBSA (kcal/Mol)**
beta.-copaene	-5.991	-69.52
Benzenebutanal, .gamma.,4-dimethyl-	-5.926	-53.47
1,6-Naphthyridine	-7.041	-38.41
Germacrene D	-4.957	-44.96
1,3-Cyclohexadiene, 5-(1,5-dimethyl-4-hexenyl)-2-methyl-, [S-(R*,S*)]-	-4.036	-54.51
beta.-Bisabolene	-5.424	-69.52
Cyclohexene, 3-(1,5-dimethyl-4-hexenyl)-6-methylene-, [S-(R*,S*)]-	-4.153	-54.49
2-Butenoic acid, 4-hydroxy-, methyl ester	-4.453	-37.75
Imidazole, 2-fluoro-5-hydroxy-1-ribofuranosyl-	-6.083	-43.14
D-Galactonic acid, .gamma.-lactone	-5.105	-24.66
beta.-D-Glucopyranoside, methyl 3,6-anhydro-	-5.340	-40.65
5-Methyl-7-amino-s-triazolo(1,5-a)pyrimidine	-7.441	-35.60
Supraene	-3.731	-57.58
Galunisertib	-10.210	-82.51

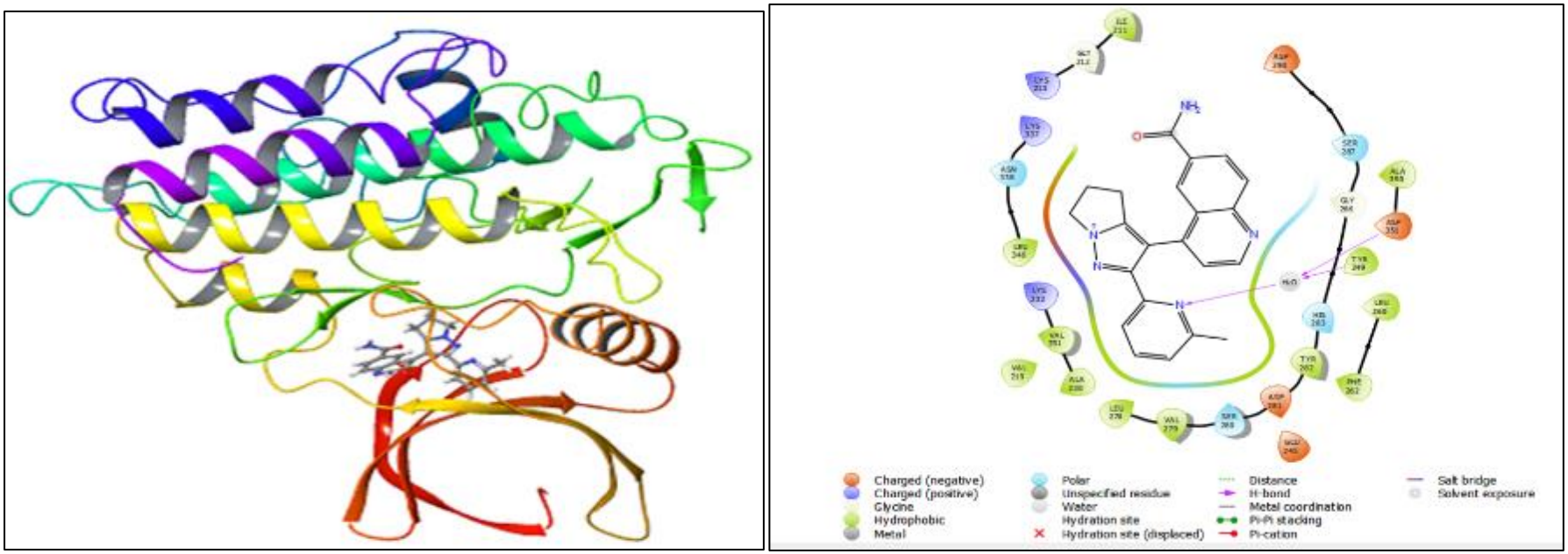

Figure 1 3 and 2D Interactions of Galunisertib (Control) with TGF-B Type I Receptor.

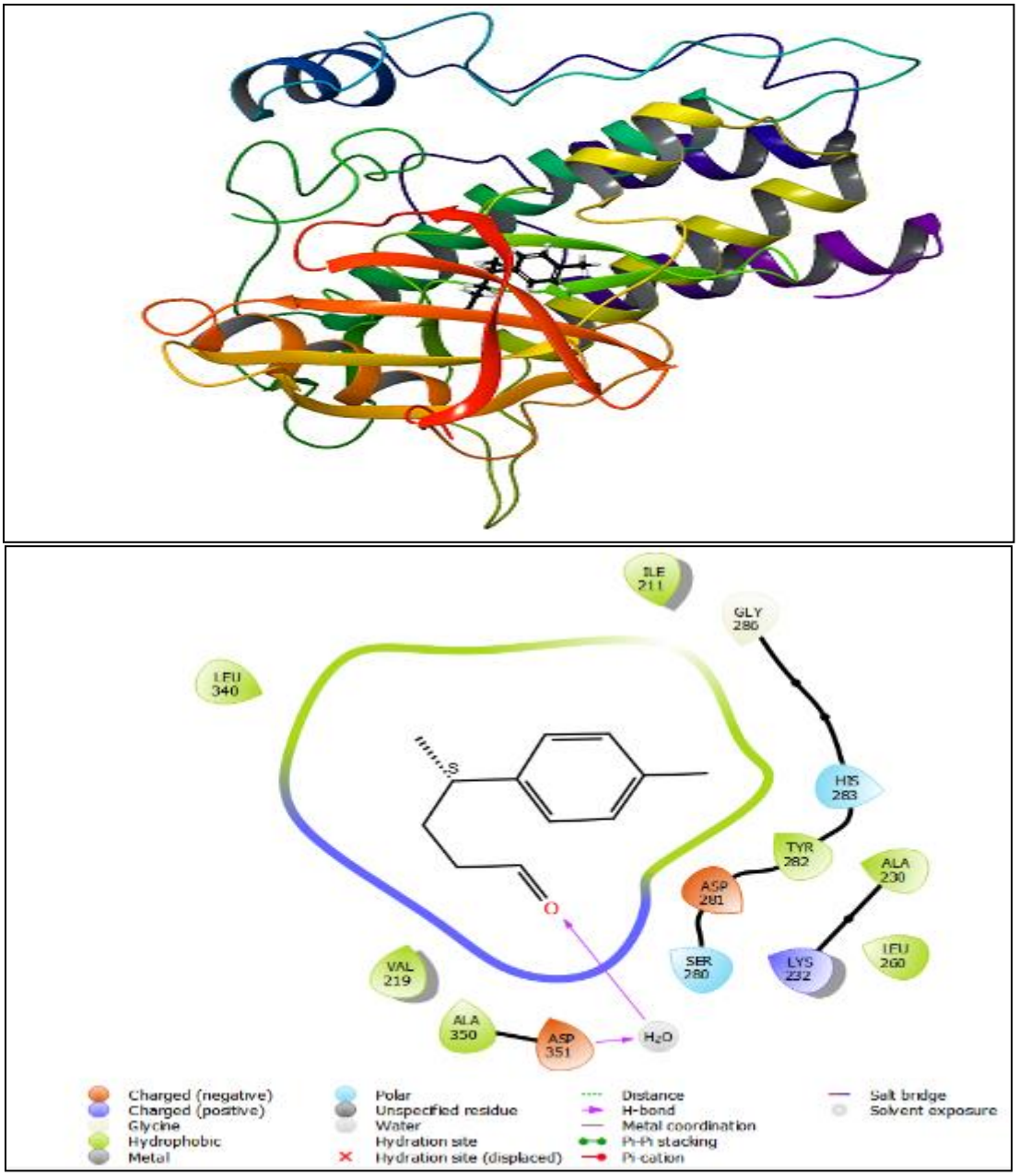

Figure 2 3 and 2D Interactions of Benzenebutanal, gamma, 4-dimethyl- with TGF-β type I receptor

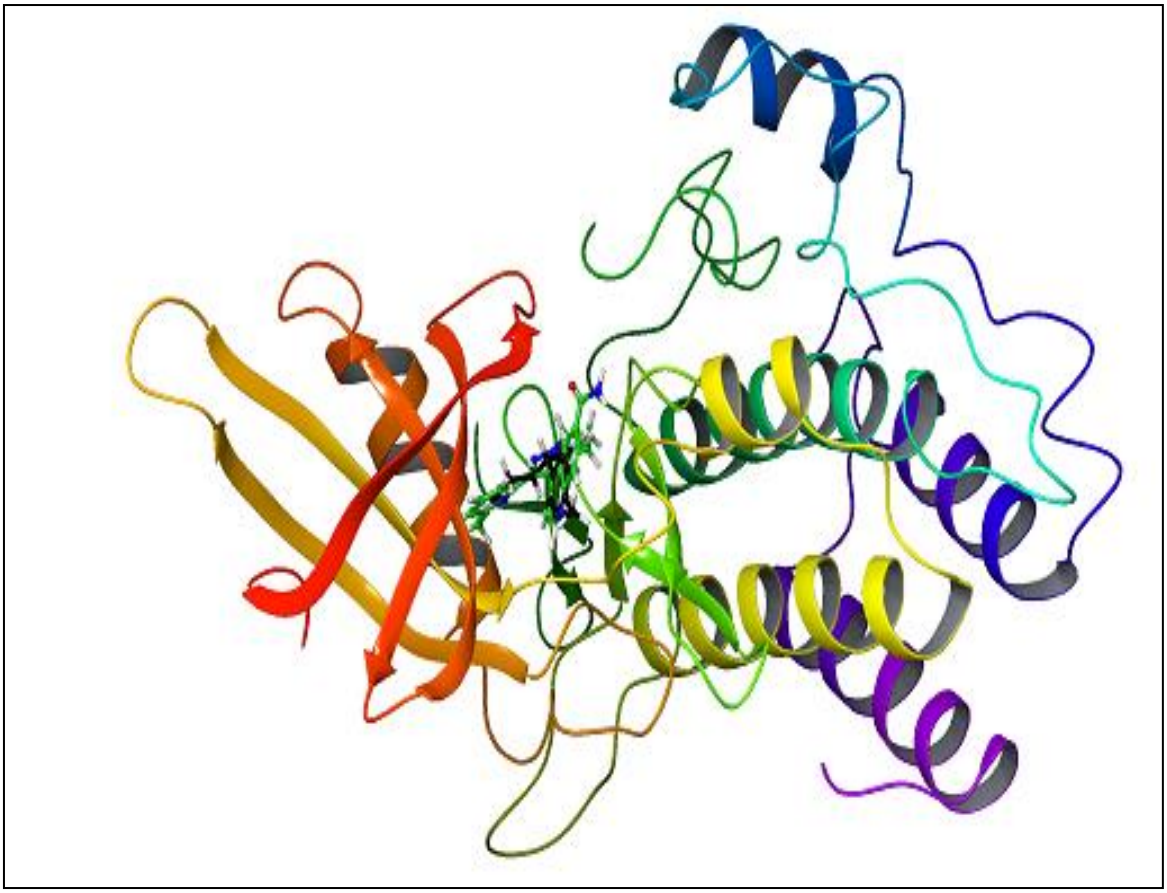

Figure 3 3-D Superimposed structure of Galunisertib (control) (green) and Benzenebutanal, gamma, 4-dimethyl-(black) with TGF-β type I receptor

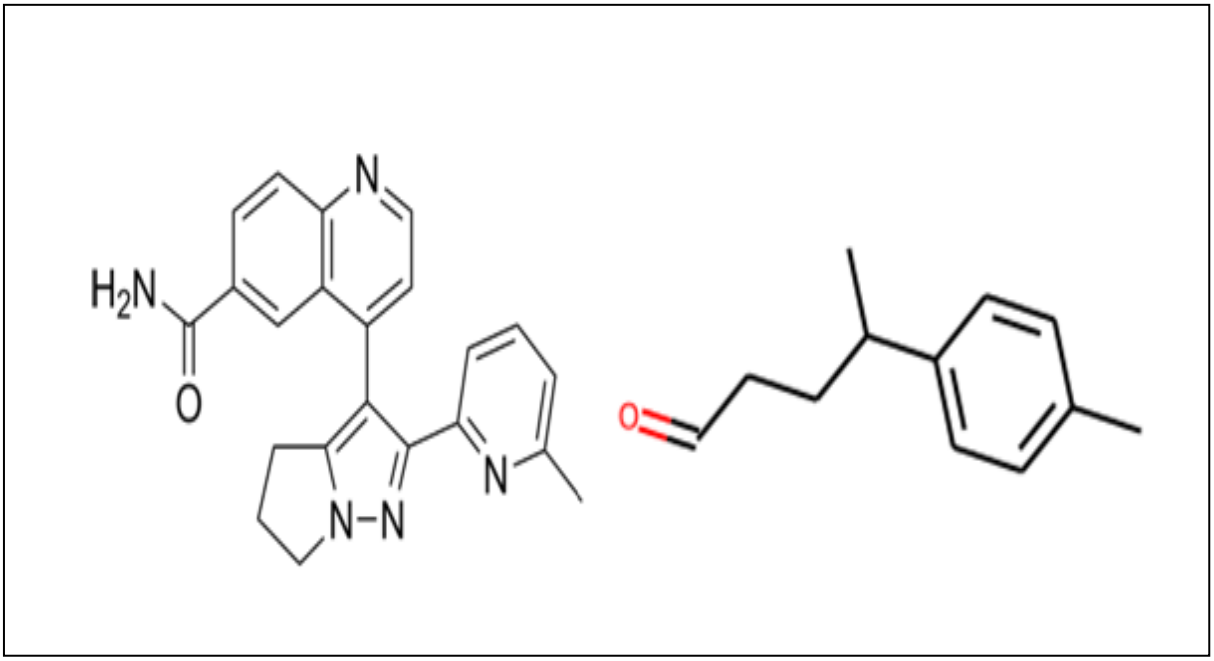

Figure 4 Structures of Galunisertib (control) and Benzenebutanal, gamma, 4-dimethyl-

4. Discussion

LD_{50} is the median lethal dose, meaning the dose at which 50% of test subjects die upon exposure to a compound. Toxicity classes also are defined according to the globally harmonized system of classification of labelling chemicals. The results suggest the possibility of the use of the extract as a potential source for the development of pharmacological agents to treat various types of ailments. The hepatotoxicity, carcinogenicity, immunotoxicity, mutagenicity and cytotoxicity parameters were predicted to find out the toxicity profile of the identified phytochemical constituents from the extract. The obtained results revealed that only two (5-Methyl-7-amino-s-triazolo (1, 5-a) pyrimidineand Germacrene D) of the compounds have a deviated carcinogenicity and immunotoxicity potential respectively, which means that the majority of the compounds are devoid of any risk of toxicity.

The main motive behind this *in silico* approach is to lower the cost and time factors involved in comparison to standard absorption, distribution, metabolism and excretion (ADME) profiling, as the *in silico* approach can screen more than 20,000 compounds within a minute; the wet laboratory will take more than 20 weeks to perform the same task (Sadeghi*et al.,* 2022). The potential of a good drug could be ruined because of the limited absorption, distribution, metabolism and excretion (ADME) characteristics (Gleeson *et al.,* 2011) Furthermore, the major drawback of drug discovery in clinical trials is believed to be its pharmacokinetic properties, by virtue of which it becomes very expensive. Therefore, ADME parameters were estimated using *in silico* tools to determine the probability of the extract becoming a potential candidate for the development of drugs.

If a ligand has a high lipophilicity (less than 5) it may also be regarded as drug-like (Arnott and Planey, 2012). Log Po/w is the way to explain this. Most of the ligands had lipophilicity values that were less than 5, making medicines the most plausible candidates with exception of 17-Pentatriacontene and Supraene with very large values. Blood brain barrier (BBB) penetration should be kept to a minimum for medications not targeting the central nervous system (CNS) in order to prevent unfavourable side effects (Clark, 2003). Pharmacokinetically, most of the compounds had significant gastrointestinal drug absorption; however few were permeable to the blood–brain barrier (BBB) (1-Decanol 2-ethyl-Hexadecanoic acid methyl ester, Oxalic acid cyclobutyltridecyl ester and 2-Pentadecanol). The role of the plasma membrane ATP-binding cassette transporter known as P-glycoprotein (P-gp) affects the drug transport process. The activation of P-gp results in the efflux of the drug outside the cells, so the therapeutic effect is not achieved (Ojo *et al.,* 2021).In the present study, most tested ligands were not substrate to P-gp, thus indicating their bioavailability in the cells with exception of Pentane-1,2,3,4,5-pentaol and 17-Pentatriacontene.

Drug-like and non-drug-like compounds can be distinguished using Lipinski's rule of five (Lipinski, 2004). These filters aid in the early stages of preclinical development and may help to prevent expensive late-stage preclinical and clinical failures. The rule states that, orally active drugs in general must not violate more than one of the following criteria: the hydrogen bond donors must not be more than 5 (the summation of nitrogen–hydrogen and oxygen–hydrogen bonds), hydrogen bond acceptors must not exceed 10 (all nitrogen or oxygen atoms), the molecular mass of the compound must be less than 500 Da, an octanol water partition coefficient (log P) must not exceed 5 (Leo *et al.,* 1971). Since most of the tested compounds broke just one of the Lipinski's criteria, they are all likely to be medicines (Table 3).

The distributed drug is then metabolized by CYP450 and xenobiotic in the liver and intestines. The foremost clinically appropriate drug-metabolizing enzyme in the human body is CYP3A4. It is responsible for the metabolism of about 60% of xenobiotic, including drugs, carcinogens, steroids and eicosanoids. When a compound is found as a substrate for at least one type of CYP450 enzyme, then the compound is anticipated to be easily metabolized by the respective CYP450 enzyme (Zhao, *et al.,* 2021).This is evident as the most compounds were found to be substrates to CYP450 enzyme.

In the molecular docking analysis, the GC-MS profile of ethanol fruit extract of *Raphia hookeri* revealed few compounds that performed well against TGF-β1 compared to the control drug galunisertib. Galunisertib scored a binding affinity value of -10.210 Kcal/mole, while the highest-scoring compounds were 1,6-Naphthyridine and 5-Methyl-7-amino-s-triazolo(1,5-a) pyrimidine with a docking score of -7.041 and -7.441 Kcal/mole respectively. However, other compounds such as Benzenebutanal, .gamma.,4-dimethyl-, Imidazole, 2-fluoro-5-hydroxy-1-ribofuranosyl-, D-Galactonic acid, .gamma.-lactone and beta.-D-Glucopyranoside, methyl 3,6-anhydro- possessed a relatively high docking scores of -5.926, -6.083, -5.105 and 5.340 Kcal/mole respectively. This difference may be owed to the structural disparities between these molecules and their subsequent abilities to occupy the binding pocket of the macromolecule (Table 4).

The MM-GBSA approach facilitates computation of free energies of binding and ranking of series of ligands (Rastelli *et al*., 2010; Sgobba *et al*., 2012). This approach was used to further validate the choice of the most probable binding site of the ligands on the 1vjy structure. The ensemble-average MM/GSBA rescoring was further performed for some selected docking poses. As expected, MM/GBSA rescoring ranks of the poses differently than the docking method because the docking program uses an empirical scoring function as more like "machine learning" than direct physics-based in nature (Rastelli *et al.,* 2010; Sgobba *et al.,* 2012). Thus, the ranks of the poses from two methods could differ significantly. The MM/GBSA method is considered to be more accurate at the cost of computer time. The top docking ranked poses are the lowest ranked poses using MM/GBSA rescoring, indicating the very importance of keeping a few top poses for rescoring (Zhang *et al*., 2017). In this study, beta.-copaene, Benzenebutanal, .gamma.,4-dimethyl- and beta.-Bisabolene posse the highest free binding energy of -69.52, -53.47 and -69.52 (kcal/mol) respectively when compared with Galunisertib (control) with -82.51(kcal/mol) (Table 5).

Galunisertib has two conjoined pentacyclic ring structures, the second of which has two branches attached to it, one of which contains a single hexacyclic ring and the other two conjoined hexacyclic rings. This unique structure allows galunisertib to form interactions via hydrogen bonds with 2 residues (Tyr249 and Asp351) in the binding pocket (fig.1). The steric configuration of Benzenebutanal, gamma, 4-dimethyl- is more similar to that of galunisertib. However, it has one cyclic structure only compared to galunisertib (fig.4). Moreover, a cyclic extension at the junction point contributes little to ligand-macromolecule interactions but likely cause steric hindrance, resulting in a lower binding affinity than the control. This is in line with the work of Tithi *et al*. (2023).

5. Conclusion

The current study of *Raphia hookeri* (Rh) *in silico* provides new insight into hepatoprotective activity. In the molecular docking and MMGBSA analysis, Benzenebutanal, gamma, 4-dimethyl revealed a good binding affinity with corresponding high MMGBSA scores and interactions with TGF-β type I receptor when compared to the Galunisertib (control). The ADME and oral toxicity study also displayed their drug-likeness characters with Benzenebutanal, gamma, 4-dimethyl penetrating the blood brain barrier (BBB).

Compliance with ethical standards

Acknowledgments

The authors have acknowledged Mrs. Regina Akighir for her various contributions to the knowledge of science and Dr. J. V. Anyam for his technical expertise throughout this work.

Disclosure of conflict of interest

The authors declared that there is no conflict of interest

Statement of ethical approval

This study was conducted in accordance with established ethical principles for research involving human/animal subjects. Ethical approval was obtained from the appropriate Ethics and Research Committee before the commencement of the study. Participation was voluntary, and confidentiality of all information obtained was strictly maintained throughout the research process.

Statement of informed consent

Written informed consent was obtained from all participants before sample collection and data acquisition, and confidentiality of all information obtained was strictly maintained throughout the study.

References

[1] Akighir, J., Yakubu, O. E., Imo, C., Ojogbane, E., Owuna, R. and Jato, J. A. (2023). Evaluation of the total antioxidant capacity, total polyphenol content, and flavonoids content in ethanolic fruit extract of Raphia hookeri and determination of the correlation between the antioxidant effects and the phytochemical contents. *International Journal of Research in Pharmaceutical Sciences* 14(3): 141-152

[2] Akpan E. J. and Usoh, F.I. (2004). Phytochemical screening and effect of aqueous root extract of Raphia hookeri (raffia palm) on metabolic clearance rate of ethanol in rabbits. *Nigerian Society for Experimental Biology*, 16(1): 37-42.

[3] Arnott, J.A. and Planey, S.L. (2012). The influence of lipophilicity in drug discovery and design. *Expert Opinion on Drug Discovery*, 7(10): 863-938.

[4] Bo, Zhang., Fanzheng, Meng., Yao, Liu., Yubin, Yuan., Jizhou, Wang., Dehai, Wu., Yifeng, Cui., Shugeng, Zhang., Hongrui, Guo., Shuhang, Liang., Wei, Wang., Matthew, Klos., Sherry, Morgenstern., Yufeng, Liu., Linmao, Sun., Kun, Ma., Xirui, Liu., Yan, Wang., Jihua, Han., Guangchao, Yang., Chenyang, Zheng., Xianying, Li., Shuo, Zhou., Changyong, Ji., Qingquan, Bai., Jiabei, Wang., Lianxin, Liu. (2021). Inhibition of TGFβ1 accelerates regeneration of fibrotic rat liver elicited by a novel two-staged hepatectomy. *Theranostics*, doi: 10.7150/THNO.52102

[5] Carlesso, A., Chintha C. and Gorman, A.M. (2019) Merits and pitfalls of conventional and covalent docking in identifying new hydroxyl aryl aldehyde like compounds as human IRE1 inhibitors. 9:3407

[6] Clark, E. C. (2003). *In silico* prediction of blood-brain barrier permeation. *Drug Discovery Today*, 8(20): 927-933.

[7] Dada, F.A., Oyeleye, S. I., Ogunsuyi, O.B., Olasehinde, T.A., Adefegha, S.A., Oboh, G. and Boligon, A.A. (2017). Phenolic constituents and modulatory effects of Raffia palm leaf (Raphia hookeri) extract on carbohydrate hydrolysing enzymes linked to type -2diabetes. *Journal of Traditional Complement Medicine,* 7(4): 4994-500.

[8] Gleeson, M.P., Hersey, A., Montanari, D. and Overington, J. (2011). Probing the Links between in Vitro Potency, ADMET and Physicochemical Parameters. *Natural Review Drug Discovery,* 10: 197–208.

[9] Halgren, T.A., Murphy R.B. and Friesne,r R.A. (2004) Glide: a new approach for rapid, accurate docking and scoring 2. Enrichment factors in database screening. *J. Med. Chem*. 47:1750–1759.

[10] Herbertz, S., Sawyer, J.S., Stauber, A.J., Gueorguieva, I., Driscoll, K.E., Estrem, S.T., Cleverly, A.L., Desaiah, D., Guba, S.C., Benhadji, K.A., Slapak, C.A. and Lahn, M.M. (2015). Clinical development of galunisertib (LY2157299 monohydrate), a small molecule inhibitor of transforming growth factor-beta signaling pathway. Drug Des Devel Ther. 10(9): 4479-99.

[11] Ipav, S. S., Igoli, . J. O., Tor-Anyiin, T. A. and Anyam, J. V. (2022). Isolation and Characterisation of Alpha and Beta Amyrins from Propolis Obtained from Benue State. *Journal of Chemical Society of Nigeria,* 47(2).

[12] Jasuja, H., Chadha, N., Kaur M. and Silakari O. (2014). Dual inhibitors of Janus kinase 2 and 3 (JAK2/3): designing by pharmacophore- and docking-based virtual screening approach. Mol. Divers. 18(2): 253–267.

[13] Leo, A., Hansch, C. and Elkins, D. (1971). Partition coefficients and their uses. *Chemical Reviews,* 71(6): 525–616.

[14] Link, F., Yujia, Li., Jieling, Z., Stefan, M., Weiguo, F., Zeribe, C., Nwosu., Y.Y., Seddik, H., Roman, L., Hui, L., Chen, S., Bing, S., Natalie, J., Huiguo, D., Matthias, P, E., Hong-Lei, W., Peter, D., Dirk, D., Steven, D. and Sai, W. (2023). Extracellular Matrix Protein 1 Attenuates Hepatic Fibrosis by Inhibiting TSP-, ADAMTS-, and MMP-Mediated Latent TGF-β1 Activation. bioRxiv, doi: 10.1101/2023.12.12.571289

[15] Lipinski, C.A. (2004) Lead- and Drug-like Compounds: The Rule-of-Five Revolution. Drug Discovery Today: *Technologies*, 1: 337-341.

[16] Lyne, P.D., Lamb, M. L and Saeh, J.C. (2006). Accurate prediction of the relative potencies of members of a series of kinase inhibitors using molecular docking and MM-GBSA scoring. J Med Chem2006;49:4805–4813

[17] Mbaka, G. O, Ogbonia, S.O., Oyeniran, K.J. and Awopetu, P.I. (2012). Effect of *Raphia hookeri* seed extract on blood glucose, glycosylated hemoglobin and lipid profile of alloxan induced diabetic rats. *British Journal of Medicine and Medical Research*, 2(4):621-635.

[18] Modi, P., Patel S. and Chhabria M. (2018). Structure-based design, synthesis and biological evaluation of a newer series of pyrazolo [1, 5-a] pyrimidine analogues as potential anti-tubercular agents. Bioorg. Chem. 87: 240–251.

[19] Ncube, N., Afolayan, S.A.J. and Okoh, A.I. (2008). Assessment techniques of antimicrobial properties of natural compounds of plant origin: current methods and future trends. *African Journal for Biotechnology,* 7(12): 1797-1806.

[20] Nguyen, V.T., Sakoff, J.A. and Scarlett, C.J. (2017). Physicochemical properties, antioxidant and cytotoxic activities of crude extracts and fractions from *Phyllanthus amarus. Medicines*, 4(2), 42.

[21] Ojo, O.A., Ojo, A.B., Okolie, C., Nwakama, M.C., Iyobhebhe, M., Evbuomwan, O., Nwonuma, C.O., Maimako, R.F., Adegboyega, A. E.,Taiwo, O.A., Alsharif, K.F and Batiha, G.E. (2021). Deciphering the Interactions of Bioactive Compounds in Selected Traditional Medicinal Plants against Alzheimer's Diseases via Pharmacophore Modeling, Auto-QSAR, and Molecular Docking Approaches. *Molecules,* 26 (7), 1996.

[22] Pradeep, H. and Rajanikant G.K. (2012). A rational approach to selective pharmacophore designing: an innovative strategy for specific recognition of Gsk3b, 16(3):553–562.

[23] Rastelli, G., Del Rio, A., Degliesposti, G. and Sgobba, M. (2010). Fast and accurate predictions of binding free energies using MM-PBSA and MM-GBSA. *J. Comput. Chem.*, *31*, 797– 810, DOI: 10.1002/jcc.21372

[24] Sadeghi, M., Miroliaei, M., Fateminasab, F. and Moradi, M. (2022). Screening cyclooxygenase-2 inhibitors from *Allium sativum L*. compounds: in silico approach. *Journal of Molecular Modelling,* 28: 1-12

[25] Schon, H.T. and Weiskirchen, R. (2014). Immunomodulatory effects of transforming growth factor-β in the liver. Hepatobiliary Surg. Nutr. 3: 386–406.

[26] Sgobba, M.; Caporuscio, F.; Anighoro, A.; Portioli, C.; Rastelli, G. (2012). Application of a post-docking procedure based on MM-PBSA and MM-GBSA on single and multiple protein conformations. *Eur. J. Med. Chem.*, *58*, 431– 440.

[27] Sinha, S., Patel, S. and Mohd, A. (2019). Structure-based identification of novel sirtuin inhibitors against triple negative breast cancer: an in silico and in vitro study. 140:454–468.

[28] Subramaniyan, V., Palani M. and Srinivasan, P. (2018). Novel ligand-based docking; molecular dynamic simulations; and absorption, distribution, metabolism, and excretion approach to analyzing potential acetylcholinesterase inhibitors for Alzheimer's disease. J Pharmacological Analgesics 8: 413–420

[29] Thomas, E., T.P. Aneesh, D.G. Thomas and R. Ananda, 2013. GC-MS analysis of phytochemical compounds present in rhizomes of Nervilia aragoana gaud. *Asian Journal of Pharmacology and Clinical Research,* 6: 68-74.

[30] Thomas, G., Bird., Thomas, G., Bird., Miryam, Müller., Luke, Boulter., David, F., Vincent., Rachel, A., Ridgway., Elena, Lopez-Guadamillas., Wei-Yu, Lu., Thomas, Jamieson., Olivier, Govaere., Andrew, D., Campbell., Sofia, Ferreira-Gonzalez., Alicia, M., Cole., Trevor, Hay., Kenneth, J., Simpson., William, Clark., Ann, Hedley., Mairi, Clarke., Pauline, Gentaz., Colin, Nixon., Steven, A., Bryce., Christos, Kiourtis., Joep, Sprangers., Robert, J., B., Nibbs., Nico, van, Rooijen., Laurent, Bartholin., Steven, R., McGreal., Udayan, Apte., Simon, T., Barry., John, P., Iredale., John, P., Iredale., Alan, Richard, Clarke., Manuel, Serrano., Tania, Roskams., Owen, J., Sansom., Stuart, J., Forbes., Stuart, J., Forbes. (2018). TGFβ inhibition restores a regenerative response in acute liver injury by suppressing paracrine senescence. Science Translational Medicine, doi: 10.1126/SCITRANSLMED.AAN1230

[31] Tithi TI, Tahsin M.R, Anjum J, Zaman TS, Aktar F, Bahar NB, et al. (2023) An in vivo and in silico evaluation of the hepatoprotective potential of Gynura procumbens: A promising agent for combating hepatotoxicity. PLoS ONE 18(9): e0291125. https://doi.org/10.1371/journal. pone.0291125

[32] Xudong, S., Jiayi, S., Jieting, L., Yong, L., Yang, Y., Yu-ming, Q., Zhi-xin, C., Yu, P., Xiaohuan, Y., Yanhui, C. and Dan, W. (2022). Recombinant truncated latency-associated peptide alleviates liver fibrosis in vitro and in vivo via inhibition of TGF-β/Smad pathway. *Molecular Medicine,* doi: 10.1186/s10020-022-00508-2.

[33] Yakubu, O.E., Nwodo, O.F.C., Joshua, P.E., Ugwu, M.N., Odu, A.D. and Okwo, F. (2014). Fraction and determination of total antioxidant capacity, total phenolic and total flavanoid contents of aqueous, ethanol and n-hexane extracts of *vitex doniana* leaves. *African Journal for Biotechnology,* 13(5): 693-698.

[34] Yakubu, E.O, Boyi, R.N., Shaibu, C., Abu, M., and Akighir, J. (2019). Antioxidant Parameters and GC-MS phytochemical Analysis of *Hymenocardia acida* stem Bark Ethanolic Extract. *Trend in Applied Science Research,* (14): 263-270.

[35] Zhang, X., Perez-Sanchez, H. and Lightstone, F.C. (2017). A Comprehensive Docking and MM/GBSA Rescoring Study of Ligand Recognition upon Binding Antithrombin. *Curr Top Med Chem*. 17(14):1631-1639.

[36] Zhao, M., Ma, J., Li, M., Zhangm, Y., Jiang, B., Zhao, X., Huaim C., Shenm L., Zha ngm, N., He, L. and Qin, S. (2021). Cytochrome P450 Enzymes and Drug Metabolism in Humans. *International Journal of Molecular Sciences*, 26; 22(23): 12808.